52nd IEEE Conference on Decision and Control
December 10-13, 2013. Florence, Italy

Enhancing Distribution Networks to Evolve toward Smart Grids: the Voltage Control Problem

Anna R. Di Fazio, *Member, IEEE,* Giuseppe Fusco, *Member, IEEE,* and Mario Russo, *Member, IEEE*

***Abstract*— The evolution of existing distribution systems toward smart grids requires the exploitation of all the capabilities of the new Distributed Generation (DG). To this aim, the present paper addresses the problem of improving the voltage profile regulation in distribution networks with DG. According to a decentralized approach, the set-point of a reactive power regulation scheme of the DG is designed in an optimal sense by solving a constrained minimization problem. Since the proposed design uses only local measurements new investments on the existing networks are limited. The results of numerical simulations are provided for a MV multiple–feeder distribution system with multiple DGs with reference to two different optimization objectives.**

I. Introduction

In the development of smart distribution grids, microgrids have been pointed out as a reference structure because of their high flexibility and scalability [1]. A microgrid is a modest-size, self sustained and controlled unit of the distribution system which aggregates renewable generation, energy storages and active demand. Microgrids interact by exchanging energy and services through the distribution network.

However, in a medium term horizon, the advent of smart distribution grids will not take place by a revolution and it is unquestionable that the main problem is to gradually evolve from the existing distribution system to the smart grid of the future [2]. While the ex-novo design of a distribution system can be realized with integrated microgrids, the existing networks present an inflexible structure, inadequate to allow a large penetration of distributed energy resources and to promote market competition in the electrical sector. Then, nowadays, research should focus on the way to override these obstacles and remove technical and economical barriers to achieve the smart grid vision.

In this road-map towards innovation, addressing the voltage regulation problem of smart MV distribution systems represents a key issue to maintain satisfactory voltage levels in the grid. The first concern in this research field has been to analyze the impact of Distributed Generation (DG) on the voltage profile of existing distribution systems. It has been shown how the interaction between the On-Load Tap Changer (OLTC) in the HV/MV substation and the DG may cause over or undervoltages along the feeders, especially in presence of Line Drop Compensation (LDC) [3]–[5].

To allow a larger penetration of renewable DGs, while keeping an adequate voltage profile along the distribution feeders by managing the reactive power, new control systems have been proposed in the literature, adopting centralized or decentralized approaches. Centralized approaches require significant investment in sensors, communications, and control systems [6]–[8], which makes their application to massive DG situations difficult to implement. Conversely, in a decentralized approach, the control actions are locally determined and communication is required only for coordination purpose. Such a coordination can be performed either on-line, by adequate chains of command typically based on multi-agent techniques [9]–[11], or off-line at the design stage [8], [12]–[14]. The off-line coordination avoids any modification of the architecture of existing control systems and any significant investment for additional measurements. Moreover, data exchange is needed only in the case of significant changes of the distribution system structure.

Aiming at significantly reducing the impact on the existing networks as well as to limit new investment, this paper proposes a decentralized approach to optimize the voltage profile along the feeders of the distribution system. The idea is to to design the set-point of the DG reactive power closed loop control scheme in an optimal sense. This idea, previously introduced in [15], is that each local controller of a DG optimizes the voltage profile of a feeder or an area of the distribution system, which is assigned to the specific controller by an off-line coordination. The main features of the proposed optimization design are the following ones: 1) it requires only local measurements at the Point of Common Coupling (PCC); 2) it can be applied to any classical DG control scheme, whichever the regulated variable; 3) it takes into account the changes of the feeder loading conditions as well as of the operating conditions of the feeder supplying system; 4) the communication needs are limited to the events of network structural changes. In the newly proposed approach the reference value of the reactive power closed loop control scheme is designed by solving a constrained minimization problem. The proposed technique uses an estimation of the operating conditions of the primary substation and of the loads to minimize an assigned function of the voltage amplitude at each node of the feeder. Extensive numerical simulations give evidence of the improvements of the feeder voltage profile.

II. Distribution system model

Let the generic MV distribution system shown in Fig. 1 be considered, composed of a supplying system and various feeders including DGs. In the following a model of the distribution system is presented which is suitable to the development of the optimal set-point design presented in the next Section. Then, let us focus on a generic DG connected at the busbar m of a feeder with n nodes.

A.R. Di Fazio, G. Fusco and M. Russo are with the Dipartimento di Ingegneria Elettrica e dell'Informazione, Università degli Studi di Cassino e del Lazio Meridionale, Cassino, FR, 03043 Italy, e-mail: fusco@unicas.it.

978-1-4673-5716-6/13/$31.00 ©2013 IEEE

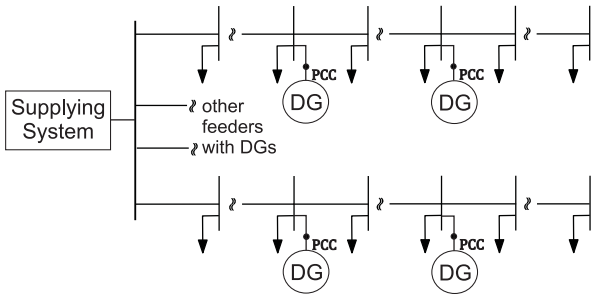

Fig. 1. Single-line representation of the MV distribution system composed of multiple feeders and DGs.

Concerning the supplying system, it is modelled by the Thevenin equivalent circuit as seen from the MV busbar 0. The no-load voltage generator $\bar{v}_{sub}$ and the leakage impedance $\bar{z}_{sub}$ may vary in amplitude and phase due to the changes of the supplying system operating conditions. In the following, a simplified model is adopted in which $\bar{z}_{sub}$ does not change and all the changes of the operating conditions are modelled by variations of $\bar{v}_{sub}$.

The generic i-th load L_i is modeled by an equivalent shunt admittance

$$\bar{y}_{Li} = \bar{k}_{Li}\, \bar{y}_{load} \tag{1}$$

where $\bar{k}_{Li}$ is a load factor which represents the contribution of $\bar{y}_{Li}$ in the total equivalent load admittance $\bar{y}_{load}$. All $\bar{k}_{Li}$ are assumed to be known and constant while variations of the loads are taken into account by changing the value of $\bar{y}_{load}$. If all the loads L_i present the same power factor, $\bar{k}_{Li}$ are real constants.

The DG is represented by current injections $\bar{I}_{pcc}$ depending on the active and reactive powers P_{pcc} and Q_{pcc} injected into the network at the Point of Common Coupling (PCC) and on the nodal voltage $\bar{V}_m$ according to

$$\bar{I}_{pcc} = \frac{P_{pcc} - jQ_{pcc}}{\bar{V}_m^{\star}} \tag{2}$$

where * stands for the complex conjugation. Such a model is general and not related to the type of electric devices and/or of renewable energy source.

Concerning the MV distribution network the configuration is assumed to be known and composed of multiple radial feeders. The generic i-th line l_i is modeled by a series impedance $\bar{z}_{l_i}$, which is assumed to be known.

The other feeders connected at the supplying MV busbar 0 are modeled by an admittance $\bar{y}_{L0}$, which is equivalent to the series and parallel combinations of the line impedances and of the load admittances of the feeders. As in (1), it is assumed $\bar{y}_{L0} = \bar{k}_{L0}\, \bar{y}_{load}$.

In the above assumptions, the single-phase electric circuit in Fig. 2 represents the distribution system in Fig. 1 as seen from the PCC of the considered DG.

III. Optimal Set-Point Design

The OSPD is developed referring to the most common case of DG exploiting renewable variable source. The injected active power varies according to the availability of the primary energy source and cannot be dispatched. The injected reactive power varies due to the action of a DG

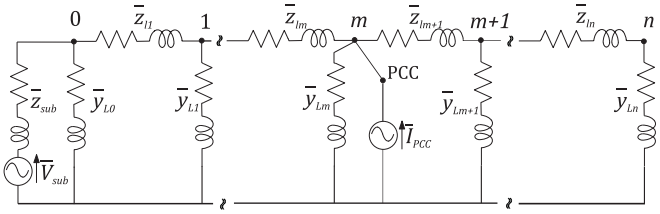

Fig. 2. Electric circuit of the distribution system from the PCC of the generic DG

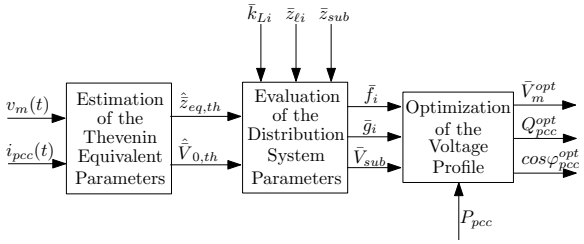

Fig. 3. Block diagram of the three steps composing the OSPD.

control scheme, which acts on the electric machine or on the power electronic converter. The DG control scheme regulates either the voltage amplitude or the injected reactive power or the power factor at the PCC, so as to keep the regulated variable equal to a set point.

Using only local measurements at the PCC as inputs, the proposed OSPD optimizes the voltage profile along the feeder by generating the optimal set-point of the DG control scheme. Figure 3 shows the block diagram of the OSPD, evidencing three steps. In the first step the parameters of the Thevenin equivalent circuit as seen from the PCC are estimated. In the second step, for each node of the feeder, the parameters of the distribution system model are evaluated. In the third step a minimization problem, optimizing the voltage profile along the feeder, is solved.

A. Estimation of the Thevenin equivalent parameters

The first step estimates the parameters of the Thevenin equivalent circuit as seen from the PCC by Kalman filters and a Constrained Recursive Least-Squares (CRLS) algorithm. Using the measures of the nodal voltage $v_m(t)$ and of the total current $i_{pcc}(t)$ injected by the DG, the Kalman filters reconstruct the corresponding phasors $\bar{V}_m$ and $\bar{I}_{pcc}$. Using these phasors, the CRLS estimates the Thevenin equivalent impedance $\widehat{\bar{z}}_{eq,th}$ and the no-load voltage $\widehat{\bar{V}}_{0,th}$. Details about the algorithms are reported in [16], [17].

B. Evaluation of the distribution system parameters

From the electric circuit in Fig. 2, the nodal voltage profile along the feeder can be expressed by the set

$$\bar{V}_i = \bar{f}_i\, \bar{V}_{sub} + \bar{g}_i\, \bar{I}_{pcc} \quad i = 1, \ldots n \tag{3}$$

where $\bar{V}_i$ is the i-th nodal voltage. The second step of the OSPD evaluates, firstly, the parameters $\bar{f}_i$ and $\bar{g}_i$, which are complex parameters depending on all the impedances in the electric circuit, and, secondly, the enforcement $\bar{V}_{sub}$.

The parameters $\bar{f}_i$ and $\bar{g}_i$ can be calculated using the classical electric circuit theory for reducing series and parallel impedances and for voltage partitions, if all the impedances

of the electric circuit in Fig. 2 are known. Being the line impedances $\bar{z}_{\ell i}$ assigned as well as the supplying system impedance $\bar{z}_{sub}$, the only unknown impedances are $\bar{y}_{Li}$ related to the loads. Standing (1) and being $\bar{k}_{Li}$ given, the only unknown impedance results to be $\bar{y}_{load}$: it can be evaluated using the estimated value $\widehat{\bar{z}}_{eq,th}$. Unfortunately, the relationship between $\bar{y}_{load}$ and $\widehat{\bar{z}}_{eq,th}$ is not explicit and requires the numerical solution of a non linear problem. The use of look-up tables can improve computational efficiency of the solving algorithm. Such tables can be filled at the design stage by numerically solving the non linear problem for various values of $\widehat{\bar{z}}_{eq,th}$. In operation, using the estimated value $\widehat{\bar{z}}_{eq,th}$ as entry to the appropriate look-up table, the total load admittance $\bar{y}_{load}$ is obtained. To account for expected variations of the load factors $\bar{k}_{Li}$, for example during a day, different pre-calculated look-up tables can be stored by OSPD.

The parameter $\bar{V}_{sub}$ can be evaluated using $\widehat{\bar{V}}_{0,th}$. In fact, the estimates $\widehat{\bar{z}}_{eq,th}$ and $\widehat{\bar{V}}_{0,th}$ can be related to $\bar{V}_m$

$$\bar{V}_m = \widehat{\bar{V}}_{0,th} + \widehat{\bar{z}}_{eq,th}\, \bar{I}_{pcc} \tag{4}$$

and, comparing (4) with (3) for $i = m$ yields

$$\bar{V}_{sub} = \frac{\widehat{\bar{V}}_{0,th}}{\bar{f}_m} \quad \text{and} \quad \bar{g}_m = \widehat{\bar{z}}_{eq,th} \tag{5}$$

C. Optimization of the voltage profile

The third step evaluates the optimal set-point for the DG voltage/reactive power control scheme on the basis of the distribution system parameters and of the measure of the injected active power. The voltage profile optimization is formulated as a minimization problem subject to power flow and voltage constraints. Various objective functions can be adopted based either on the deviations from a reference profile [7], [18] or on the distribution system losses [12], [13]. In this paper it is assumed a general objective function J which is a function of the nodal voltages along the feeder. The optimization problem is

$$\min J(\bar{V}_i) \tag{6}$$

$$\text{s. t.} \qquad \text{equations (2), (3) and}$$
$$V^m \le V_i \le V^M \quad i = 1, \dots n$$

where $[V^m, V^M]$ represents the allowed range of variation of nodal voltage amplitudes V_i.

To easily solve problem (6), each nodal voltage $\bar{V}_i$ in constraints (3) is expressed as function of the voltage $\bar{V}_m$ at the PCC. By substituting into (3) the expression of $\bar{I}_{pcc}$ derived from (4) and using (5), constraints (3) are rewritten as

$$\bar{V}_i = \bar{\mu}_i\, \bar{V}_{sub} + \bar{\alpha}_i\, \bar{V}_m \quad i = 1, \dots n \tag{7}$$

being

$$\bar{\mu}_i = \bar{f}_i - \frac{\bar{g}_i \bar{f}_m}{\bar{g}_m}\,, \qquad \bar{\alpha}_i = \frac{\bar{g}_i}{\bar{g}_m} \tag{8}$$

It can be proved that $\bar{\mu}_i = 0$ for $i = m, \dots n$.

In the same way, the constraint (2) is expressed as a function of $\bar{V}_m$

$$P_{pcc} - \jmath\, Q_{pcc} = \bar{V}_m^{\star}\, \frac{\bar{V}_m - \bar{f}_m \bar{V}_{sub}}{\bar{g}_m} = \frac{V_m^2 - \bar{V}_m^{\star}\, \bar{f}_m \bar{V}_{sub}}{\bar{g}_m} \tag{9}$$

The constrained minimization problem (6) is rewritten in the variables $\bar{V}_m$ and Q_{pcc} by substituting constraints (7) into J, yielding

$$\min_{\bar{V}_m, Q_{pcc}} \qquad J(\bar{V}_m) \tag{10}$$

$$\text{s. t.} \qquad \text{equation (9) and}$$
$$V^m \le \sqrt{\mathrm{Re}\{\bar{\mu}_i \bar{V}_{sub} + \bar{\alpha}_i \bar{V}_m\}^2 + \mathrm{Im}\{\bar{\mu}_i \bar{V}_{sub} + \bar{\alpha}_i \bar{V}_m\}^2} \le V^M$$

The constraint (9) can be split in its real and imaginary parts. The real part of (9) is a function of only $\bar{V}_m = V_{m,R} + \jmath V_{m,I}$ and is expressed as

$$V_m^2 \; - \; \frac{\mathrm{Re}\{\bar{f}_m \bar{V}_{sub}\, \bar{g}_m^{\star}\}}{g_{m,R}}\, V_{m,R} - \frac{\mathrm{Im}\{\bar{f}_m \bar{V}_{sub}\, \bar{g}_m^{\star}\}}{g_{m,R}}\, V_{m,I} \; - \; \frac{g_m^2}{g_{m,R}}\, P_{pcc} = 0 \tag{11}$$

being $\bar{g}_m = g_{m,R} + \jmath\, g_{m,I}$ and P_{pcc} an available measure. The imaginary part of (9) is

$$Q_{pcc} \; = \; \frac{g_{m,I}}{g_m^2}\, V_m^2 - \frac{\mathrm{Re}\{\bar{f}_m \bar{V}_{sub}\, \bar{g}_m^{\star}\}}{g_m^2}\, V_{m,I} \; + \; \frac{\mathrm{Im}\{\bar{f}_m \bar{V}_{sub}\, \bar{g}_m^{\star}\}}{g_m^2}\, V_{m,R} \tag{12}$$

which provides Q_{pcc}, once $\bar{V}_m$ is known. Then, Q_{pcc} is a dependent variable and problem (10) is reformulated as a two-dimensional constrained minimization problem in the only real variables $V_{m,R}$ and $V_{m,I}$

$$\min_{V_{m,R}, V_{m,I}} \qquad J(V_{m,R}, V_{m,I}) \tag{13}$$

$$\text{s. t.} \qquad \text{equation (11) and}$$
$$V^m \le \sqrt{\mathrm{Re}\{\bar{\mu}_i \bar{V}_{sub} + \bar{\alpha}_i \bar{V}_m\}^2 + \mathrm{Im}\{\bar{\mu}_i \bar{V}_{sub} + \bar{\alpha}_i \bar{V}_m\}^2} \le V^M$$

It is apparent that constraint (11) represents a circumference in the cartesian plane, with center $O' = (a/2,\, b/2)$ and radius r, being

$$a \; = \; \frac{\mathrm{Re}\{\bar{f}_m \bar{V}_{sub}\, \bar{g}_m^{\star}\}}{g_{m,R}} \qquad b = \frac{\mathrm{Im}\{\bar{f}_m \bar{V}_{sub}\, \bar{g}_m^{\star}\}}{g_{m,R}}$$

$$r \; = \; \sqrt{\frac{a^2}{4} + \frac{b^2}{4} + \frac{g_m^2\, P_{pcc}}{g_{m,R}}}$$

Taking advantage from this property, problem (13) can be transformed into a mono-dimensional minimization problem, by changing the coordinate frame as shown in Fig 4. The cartesian coordinates $(V_{m,R}, V_{m,I})$ are replaced by the polar coordinates (ρ, δ) defined in a new frame whose origin coincides with the center O', according to

$$\bar{V}_m = V_{m,R} + \jmath V_{m,I} = \left(\frac{a}{2} + \rho\, \cos\delta\right) + \jmath \left(\frac{b}{2} + \rho\, \sin\delta\right) \tag{14}$$

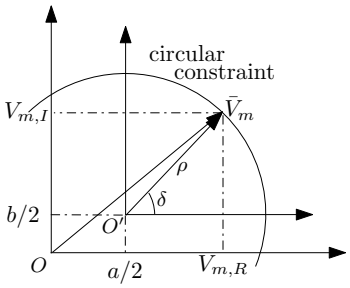

Fig. 4. Change of coordinate frame.

In this translated polar frame, constraint (11) is expressed as $\rho = r$ and it can be directly substituted into (14)

$$\bar{V}_m = V_{m,R} + \jmath V_{m,I} = \left(\frac{a}{2} + r\,\cos\delta\right) + \jmath\left(\frac{b}{2} + r\,\sin\delta\right) \tag{15}$$

Substituting (15) for $\bar{V}_m$ in problem (13), the constraint (11) is incorporated into the objective function J and it is obtained the following one-dimensional minimization problem in the variable δ

$$\min_{\delta} \qquad J(\delta) \tag{16}$$

$$\text{s.t.} \quad \delta^m \le \delta \le \delta^M \tag{17}$$

The boundary values in (17) are obtained in the following way. The box constraints in problem (13) are rewritten by substituting (15) for $\bar{V}_m$

$$V^m \le \sqrt{c_{0,i} + c_{1,i}\cos\delta + c_{2,i}\sin\delta} \le V^M \tag{18}$$

where

$$c_{0,i} = \left(\mathrm{Re}\{\bar{\mu}_i\,\bar{V}_{sub}\} + \frac{a}{2}\,\alpha_{i,R} - \frac{b}{2}\,\alpha_{i,I}\right)^2 + \alpha_i^2\,r^2 + \left(\mathrm{Im}\{\bar{\mu}_i\,\bar{V}_{sub}\} + \frac{b}{2}\,\alpha_{i,R} + \frac{a}{2}\,\alpha_{i,I}\right)^2$$

$$c_{1,i} = 2\,r\left(\alpha_{i,R}\,\mathrm{Re}\{\bar{\mu}_i\,\bar{V}_{sub}\} + \alpha_{i,I}\,\mathrm{Im}\{\bar{\mu}_i\,\bar{V}_{sub}\} + \frac{a}{2}\,\alpha_i^2\right)$$

$$c_{2,i} = 2\,r\left(-\alpha_{i,I}\,\mathrm{Re}\{\bar{\mu}_i\,\bar{V}_{sub}\} + \alpha_{i,R}\,\mathrm{Im}\{\bar{\mu}_i\,\bar{V}_{sub}\} + \frac{b}{2}\,\alpha_i^2\right)$$

To map the boundary values in (18) into δ variable, the closed-form analytic solution of the following equation

$$c_{0,i} + c_{1,i}\cos\delta_i^{lim} + c_{2,i}\sin\delta_i^{lim} = (V^{lim})^2 \tag{19}$$

is obtained in the unknown δ_i^{lim}. Substituting into (19) for V^{lim} once V^m and then V^M yields n couples of limits (δ_i^m, δ_i^M). Finally, in (17) the value δ^m is determined as $\max\{\delta_i^m\}$ and the value δ^M as $\min\{\delta_i^M\}$.

The solution δ^{opt} of problem (16)-(17) is obtained by classical numerical algorithms, starting from the following initial value

$$\delta^{init} = tg^{-1}\left(\frac{\mathrm{Im}\{\bar{f}_m\bar{V}_{sub}\} - b/2}{\mathrm{Re}\{\bar{f}_m\bar{V}_{sub}\} - a/2}\right)$$

which corresponds to setting $\angle\bar{V}_m^{init} = \angle\widehat{\bar{V}}_{0,th}$.

Once δ^{opt} is obtained, it is replaced into (15) to obtain the optimal voltage $\bar{V}_m^{opt}$. The modulus V_m^{opt} is the set-point in the case of voltage-based DG control scheme.

On the other hand, if the DG control scheme requires a reactive power set-point, Q_{pcc}^{opt} is obtained by substituting $\bar{V}_m^{opt}$ for $\bar{V}_m$ into (12). The value Q_{pcc}^{opt} must be checked with respect to the allowable range of DG reactive power, which may depend on the DG operating conditions.

Eventually, if the DG control scheme requires a power factor set-point, the value $cos\varphi_{pcc}^{opt}$ can trivially be evaluated from P_{pcc} and Q_{pcc}^{opt}.

A final consideration concerns the case of multiple DGs. In the assumption of avoiding any on-line coordination, different DGs can be equipped with the proposed OSPD only if they are "electrically distant", so as to guarantee a weak interaction among the OSPDs. It is the case of DGs connected to different feeders or the case of some actual feeders, along which it is possible to identify some areas with the following characteristics: each area represents a group of nodes whose voltages are strictly coupled and different areas are connected one to another by long distance conductors. In this case, the off-line coordination among the OSPDs is obtained by firstly identifying such areas. To this aim, some methods presented in literature can be used: in [14] "zones of influence" are identified applying ϵ-decomposition [19] to a voltage sensitivity matrix, whereas in [20], [21] "voltage load areas" are obtained by a method based on the Inherent Structure Theory of the Networks [22], [23] applied to the nodal admittance matrix. Then, the off-line coordination is completed by identifying, for each area, the DG which is the best candidate to be equipped with the OSPD and by assigning to each OSPD the task to optimize the voltage profile of its area. More details about the interaction among OSPDs and between OSPD and OLTC are reported in [15].

IV. Numerical simulation studies

Numerical simulations of the MV 50Hz distribution system shown in Fig. 5 have been performed using PSCAD/EMTDC software. Two 20kV feeders are supplied by a 24MVA transformer regulating the voltage of the MV busbar 0 at 1.02p.u.. The other characteristics of the transformer are reported in Tab. I. Both the feeders are composed of 8 nodes and their electric characteristics are reported in Tabs. II and III. The feeder #1 includes a 2.4MW Wind Turbine (WT) DG at node 4, which is equipped with the OSPD. The WT rated wind speed is equal to 12 m/s and the characteristics of the synchronous generator are reported in Tab. IV; the reactive power injected by the WT DG can vary in the range $\pm$1.71MVAr. In addition, a 1.0 MW PhotoVoltaic (PV) DG without the OSPD is connected to node 7 of the same feeder and it is assumd to operate at 80% of its rated power with constant unity power factor. The feeder #2 includes a 1.4MW PV DG connected at busbar 7, which is equipped with the OSPD and can vary its reactive power injection in the range $\pm$0.85MVAr.

In the following subsections, the results for two different objective functions assigned to the OSPDs are reported. In the first subsection the voltage profile of each feeder is optimized with respect to the rated voltage. In the second subsection the feeder distribution losses are minimized. In both cases the steady-state results obtained by the adopting the OSPDs are compared with the ones obtained by:

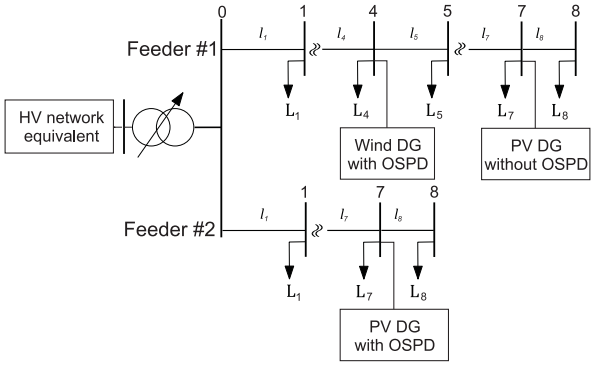

Fig. 5. Simulated distribution system with two feeders and three DGs.

- a classical control scheme in which the reactive power set-points are fixed; in particular a Unity Power Factor Control (UPFC) is considered;
- an optimization benchmark, in which a classical Optimal Reactive Power Flow (ORPF) is solved off-line for the same operating conditions.

A. Optimal voltage profile

The adopted objective function for the OSPD along each feeder is the sum of the squared differences of the nodal voltage amplitudes V_i from their reference values

$$J(\bar{V}_i) = \sum_{i=1}^{8} (V_{ref,i} - V_i)^2 \tag{20}$$

being $V_{ref,i} = 1.0 p.u.$.

Concerning the DGs operating conditions, it is assumed that the wind speed is equal to 12 m/s for the WT DG and the PV DG generates its rated active power. Concerning the loads of both feeders, two cases are considered: the peak loading conditions and the half loading conditions. For these two cases, Tabs. V and VI report the values of the reactive powers of the two DGs with OSPD and of the squared root of the objective function, $\sqrt{J}$. For the sake of comparison, the corresponding values obtained by the UPFC and by the off-line benchmark ORPF are also reported. The results show that the OSPD presents a performance which is very close to the benchmark obtained by the off-line ORPF and the voltage profiles are practically coincident since the differences in terms of the value of the objective function are very small. The improvement on the voltage profile of both the feeders achieved by the OSPD with respect to the classical UPFC is significant.

B. Minimal feeder losses

The adopted objective function for the OSPD of each feeder is

$$J(\bar{V}_i) = \sum_{i=1}^{n} \frac{r_{l_i}}{r_{l_i}^2 + x_{l_i}^2} (V_{i-1} - V_i)^2 \tag{21}$$

being $\bar{z}_{l_i} = r_{l_i} + \jmath\, x_{l_i}$.

Concerning the DGs operating conditions, it is assumed that the wind speed is equal to 11 m/s for the WT DG and the PV DG generates its rated active power. Concerning the loads of both feeders, two cases are considered: the half loading conditions and the low loading conditions, corresponding to 25 % of the peak loading conditions.

In Tabs. VII-VIII the values of the reactive powers of the two DGs with OSPD and of the total losses along the feeders are reported and compared with the corresponding values obtained by the UPFC and by the off-line benchmark ORPF. The results show that the OSPD presents a performance which is very close to the benchmark obtained by the off-line ORPF. The reduction of losses achieved by OSPD with respect to the classical UPFC control is significant.

V. Conclusion

As a first step toward smart grid realization, the paper investigates the improvements that can be achived on voltage regulation in distribution networks by exploiting DG. A decentralized optimization-based design of the set-point for the DG control scheme has been proposed. The main features of the proposed OSPD are the following ones: it requires only local measurements at the PCC; it can be applied to any classical DG control scheme, whichever the regulated variable; it takes into account the changes of the feeder loading conditions as well as of the operating conditions of the feeder

TABLE I

Data of the 132/20kV–24MVA transformer at primary substation

Type of windings	Ratio for $a = 1$	$a_{\min}$ ratio	$a_{\max}$ ratio	Reactance [p.u.]	OLTC positions
YgΔ	130/20	0.90	1.05	0.08	16

TABLE II

Data of the 20 kV–50 Hz feeders

Line name	R [Ω]	X [Ω]
l_1	0.34215	0.4806
l_2	0.34215	0.4806
l_3	0.34215	0.4806
l_4	0.34215	0.4806
l_5	0.2281	0.3204
l_6	0.2281	0.3204
l_7	0.2281	0.3204
l_8	0.2281	0.3204

TABLE III

Peak loads and rated load factors

Load name	Feeder #1 P [kW]	Feeder #1 Q [kVAr]	k_{Li}	Feeder #2 P [kW]	Feeder #2 Q [kVAr]	k_{Li}
L_1	313.0	153.0	0.0355	156.5	76.5	0.0355
L_2	313.0	153.0	0.0355	156.5	76.5	0.0355
L_3	272.5	133.35	0.0309	136.25	66.675	0.0309
L_4	272.5	133.35	0.0309	136.25	66.675	0.0309
L_5	1368.5	669.0	0.1551	684.25	334.5	0.1551
L_6	1368.5	669.0	0.1551	684.25	334.5	0.1551
L_7	2458.0	1201.85	0.2785	1229.0	600.925	0.2785
L_8	2458.0	1201.85	0.2785	1229.0	600.925	0.2785

TABLE IV

Data of the wind DG synchronous generator

Rotor type	Poles number	S [MVA]	V [kV]	H [s]	r_s [p.u.]	x_d [p.u.]
massive	2	3.0	0.69	10	0.001	1.5
x'_d [p.u.]	x''_d [p.u.]	x_q [p.u.]	x''_q [p.u.]	T'_{d0} [s]	T''_{d0} [s]	T''_{q0} [s]
0.3	0.2	1.5	0.2	6.0	0.04	0.04

TABLE V

DG REACTIVE POWERS AND OBJECTIVE FUNCTION (20) FOR THE PEAK LOADING CONDITIONS

Control Type	Feeder #1 Q_{pcc} [MVAr]	Feeder #1 $\sqrt{J}$ [10^{-3}p.u.]	Feeder #2 Q_{pcc} [MVAr]	Feeder #2 $\sqrt{J}$ [10^{-3}p.u.]
OSPD	1.71	46.5	0.24	20.3
ORPF	1.71	46.5	0.38	20.2
UPFC	0.0	61.2	0.0	21.3

TABLE VI

DG REACTIVE POWERS AND OBJECTIVE FUNCTION (20) FOR THE HALF LOADING CONDITIONS

Control Type	Feeder #1 Q_{pcc} [MVAr]	Feeder #1 $\sqrt{J}$ [10^{-3}p.u.]	Feeder #2 Q_{pcc} [MVAr]	Feeder #2 $\sqrt{J}$ [10^{-3}p.u.]
OSPD	-1.06	20.8	-0.85	23.6
ORPF	-0.66	20.4	-0.85	23.6
UPFC	0.0	21.0	0.0	52.3

TABLE VII

DG REACTIVE POWERS AND TOTAL FEEDER LOSSES (21) FOR THE HALF LOADING CONDITIONS

Control Type	Feeder #1 Q_{pcc} [MVAr]	Feeder #2 Q_{pcc} [MVAr]	Total feeders losses [kW]
OSPD	1.71	0.85	25.5
ORPF	1.71	0.85	25.5
UPFC	0.0	0.0	43.7

TABLE VIII

DG REACTIVE POWERS AND TOTAL FEEDER LOSSES (21) FOR THE LOW LOADING CONDITIONS

Control Type	Feeder #1 Q_{pcc} [MVAr]	Feeder #2 Q_{pcc} [MVAr]	Total feeders losses [kW]
OSPD	1.36	0.39	5.6
ORPF	1.14	0.50	5.4
UPFC	0.0	0.0	10.8

supplying system; the communication needs are limited to the events of network structural changes. The applicability of the proposed approach in presence of multiple DERs has also been discussed. In such cases OSPD cannot guarantee the overall loss minimization that can be obtained by acting on all the DERs installed along a feeder, but achieves the best solution that can be reached without additional measurements and communication systems. The results of numerical simulations have evidenced the performance of the proposed voltage regulation with reference to two different optimization objectives. All the results have been compared with the ones obtained by a classical DG reactive power control scheme and by an off-line optimization benchmark.

In conclusion, the proposed OS is attractive to improve the performance of present-day distribution systems, postponing the large investments required by the future smart grids. Further research will focus on the coordination among different OSPDs along the same feeder, introducing some data exchange among control systems of different DGs.

REFERENCES

[1] H. Farhangi, "The path of the smart grid," *IEEE Power & Energy Magazine*, vol. 8, no. 1, pp. 18–28, Feb. 2010.

[2] T. L. Vandoorn, B. Zwaenepoel, J. D. M. D. Kooning, B. Meersman, and L. Vandevelde, "Smart microgrids and virtual power plants in a hierarchical control structure," in *IEEE European conference on Innovative Smart Grid Technologies*, Manchester, UK, December 2011.

[3] C. Masters, "Voltage rise: the big issue when connecting embedded generation to long 11 kv overhead lines," *Power Engineering Journ.*, vol. 16, no. 1, pp. 5–12, Feb. 2002.

[4] Y. Baghzouz, "General rules for distributed generation - feeder interaction," in *Power Engineering Society General Meeting 2006*, June 2006, p. 4 pp.

[5] F. Katiraei, C. Abbey, and R. Bahry, "Analysis of voltage regulation problem for a 25 kv distribution network with distributed generation," in *Power Engineering Society General Meeting 2006*, June 2006, p. 8 pp.

[6] P. Vovos, A. Kiprakis, A. Wallace, and G. Harrison, "Centralized and distributed voltage control: impact on distributed generation penetration," *IEEE Trans. on Power Systems*, vol. 22, no. 1, pp. 476–483, Feb. 2007.

[7] A. Aquino-Lugo, R. Klump, and T. Overbye, "A control framework for the smart grid for voltage support using agent-based technologies," *IEEE Trans. on Smart Grid*, vol. 2, no. 1, pp. 173–180, Mar. 2011.

[8] P. Carvalho, P. Correia, and L. Ferreira, "Distributed reactive power generation control for voltage rise mitigation in distribution networks," *IEEE Trans. on Power Systems*, vol. 23, no. 2, pp. 766–772, May 2008.

[9] M. Baran and I. El-Markabi, "A mulitagent-based dispatching scheme for distributed generators for voltage support on distribution feeders," *IEEE Trans. on Power Systems*, vol. 22, no. 1, pp. 52–59, Feb. 2007.

[10] H. E. Farag, E. F. El-Saadany, and R. Seethapathy, "A two ways communication-based distributed control for voltage regulation in smart distribution feeders," *IEEE Trans. on Smart Grid*, vol. 3, no. 1, pp. 271–281, Mar. 2012.

[11] M. Elkhatib, R. El-Shatshat, and M. Salama, "Novel coordinated voltage control for smart distribution networks with dg," *IEEE Trans. on Smart Grid*, vol. 2, no. 4, pp. 598–605, Dec. 2011.

[12] F. Viawan and D. Karlsson, "Voltage and reactive power control in systems with synchronous machine-based distributed generation," *IEEE Trans. on Power Delivery*, vol. 23, no. 2, pp. 1079–1087, Apr. 2008.

[13] K. Tanaka, M. Oshiro, S. toma, A. yona, T. Senjyu, T. funabashi, and c. H. Kim, "Decentralised control of voltage in distribution systems by distributed generators," *IET Proc.–Gener. Transm. Distrib.*, vol. 4, no. 11, pp. 1251–1260, 2010.

[14] L. Yu, D. Czarkowski, and F. de León, "Optimal distributed voltage regulation for secondary networks with dgs," *IEEE Trans. on Smart Grid*, vol. 3, no. 2, pp. 959–967, Jun. 2012.

[15] A. R. Di Fazio, G. Fusco, and M. Russo, "Decentralized control of distributed generation for voltage profile optimization in smart feeders," *IEEE Trans. on Smart Grid*, vol. 4, no. 3, pp. 1586–1596, Sep. 2013.

[16] G. Fusco, A. Losi, and M. Russo, "Constrained least squares methods for parameter tracking of power system steady-state equivalent circuits," *IEEE Trans. on Power Delivery*, vol. 15, no. 3, pp. 1073–1080, Jul. 2000.

[17] G. Fusco and M. Russo, *Adaptive Voltage Control in Power Systems - Modeling, Design and Applications*, ser. Advances in Industrial Control. London, UK: Springer, 2007.

[18] K. Rogers, R. Klump, H. Khurana, A. Aquino-Lugo, and T. Overbye, "An authenticated control framework for distributed voltage support on the smart grid," *IEEE Trans. on Smart Grid*, vol. 1, no. 1, pp. 40–47, Jun. 2010.

[19] D. D. Šiljak, *Decentralized Control of Complex Systems*, ser. Mathematics in Science and Engineering – Vol. 184. San Diego, CA: Academic Press, 1991.

[20] G. Valtorta and et alii, "Prototypes and algorithms for network management, providing the signals sent by the DSOs to the aggregators and the markets, enabling and exploiting active demand," ADDRESS Consortium EU-FP7, Deliverable D3.1, May 2011. [Online]. Available: http://www.addressfp7.org

[21] G. M. Casolino, A. R. Di Fazio, A. Losi, and M. Russo, "Smart modelling and tools for distribution system management and operation," in *IEEE International Energy Conference & Exhibition ENERGYCON 2012*, Florence, Italy, Sep. 2012.

[22] M. A. Laughton and M. A. El-Iskandarani, "The structure of power network voltage profiles," in *7th Power Systems Computation Conference PSCC*, Lausanne, Switzerland, Jul. 1982, pp. 845–851.

[23] G. Carpinelli, A. Russo, M. Russo, and P. Verde, "Inherent structure theory of networks and power system harmonics," *IEE Proceedings on Generation-Transmission & Distribution*, vol. 145, no. 2, pp. 123–132, Mar. 1998.